

Three-Dimensional Microstructural Modelling of Wear, Crack Initiation and Growth in Rail Steel

D.I. Fletcher*, F.J. Franklin**, J.E. Garnham**, E. Muyupa**, M. Papaelias**,
C.L. Davis**, A. Kapoor*, M. Widiyarta*, and G. Vasić*

Abstract

Rolling-sliding, cyclic contact of wheel and rail progressively alters the microstructure of the contacting steels, eventually leading to micro-scale crack initiation, wear and macro-scale crack growth in the railhead. Relating the microstructural changes to subsequent wear and cracking is being accomplished through modelling at three spatial scales: (i) bulk material (ii) multi-grain and (iii) sub-grain. The models incorporate detailed information from metallurgical examinations of used rails and tested rail material. The initial 2-dimensional models representing the rail material are being further developed into 3-dimensional models. Modelling is taking account of thermal effects, and traffic patterns to which the rails are exposed.

Keywords : *Rolling contact fatigue, Ratcheting, Multi-scale model*

1. Introduction

The aim for any railway infrastructure manager is to maximize railway rail life whilst minimizing maintenance costs and ensuring high safety. One of the main factors controlling rail life is the balance between rolling contact fatigue (RCF) crack formation and wear. RCF potentially leads to catastrophic rail failure; wear results in a loss of rail profile, shortening the rail life and adversely affecting vehicle dynamics and ride quality, but can be beneficial by removing RCF cracks which have initiated at the surface. Rail grinding, usually performed to restore profile, also removes cracks at the rail surface and can be considered a form of wear, ultimately shortening the rail life. Rail steels are designed to give high resistance to RCF cracking and wear, and to provide an optimum balance between them for the expected service loading, but regular grinding is still required to remove small fatigue cracks and maintain rail profile.

Rail life prediction requires knowledge of the forces acting on (and the distribution of stresses within) the rail and an understanding of how the rail steel responds to these. The railway network is a complex system. Tracks are

often used by multiple vehicle types with different dynamics and loading characteristics, and over time these vehicles have varying wheel profiles, so wheel-rail contact data (contact patch area, shape and location and contact stress distribution) provided by multi-body vehicle dynamics simulations are at best an approximation. As more sophisticated models of the wheel-rail interface are developed, fewer simplifications and approximations are necessary in order to make rail life predictions. For example, wheel-rail contact data can be collated to represent the passage of a train, and then rail life predictions can be made about different mixtures of traffic. As another example, wheel slip at flange contact, or caused by imperfectly controlled (or uncontrolled) braking increases the temperature in the rail steel which can affect the microstructural response of the rail steel; thermal stresses also increase the severity of the contact. Model developments addressing these examples are presented below.

The ultimate aim of this work is to develop a multi-scale model which will provide guidance on rail microstructures capable of increased wear and fatigue life with more predictable operation and lower maintenance requirements. This is to be achieved by increasing the fundamental metallurgical understanding of how the different microstructural components in rails respond to loading and hence affect crack formation.

*School of Mechanical & Systems Engineering, Newcastle University, UK

**Department of Metallurgy & Materials, University of Birmingham, UK

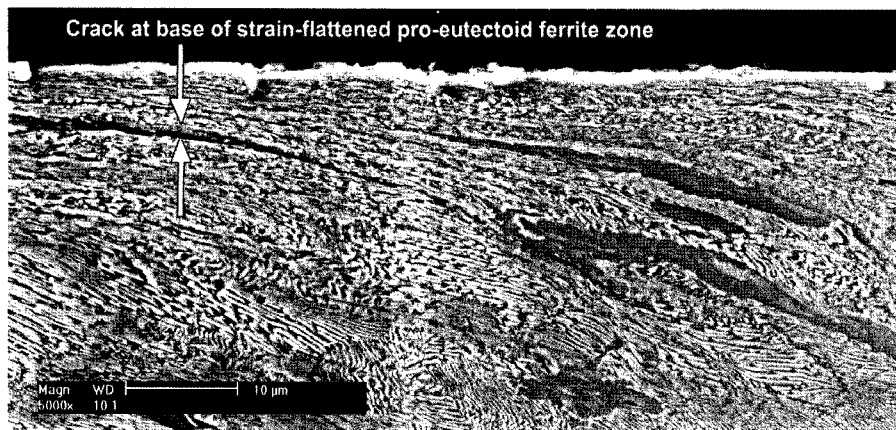


Fig. 1. RCF Crack Initiating in 220 Grade Rail Disc Tested to 25% Life. The Crack is at the Boundary between the PE Ferrite and Pearlite

2. Metallurgical Investigation

Although the mechanical properties (determined in tension) of inexpensive, low alloy, medium to high carbon, pearlitic steels are inferior to those of hardened and tempered steels usually used for bearing contacts, pearlitic microstructures are modified by the directional strain hardening generated by compressive, rolling-sliding contact so that they adequately function for wheel-rail contact. However, there is eventual strain exhaustion at and near the surface leading to micro-wear events and initiation of RCF cracks, particularly at high load, high creepage locations such as just above the gauge corner of high rails on bends.

Such contacts can be simulated to a degree by carefully controlled, twin-disc tests. Multi-angle sectioning of used rail at these locations and twin-disc testing to RCF life, and part-lives, have shown that wear, crack initiation and growth are strongly microstructurally dependent. Some rail test discs were heat-treated to maximise or minimise pro-eutectoid (PE) ferrite content and it was clearly established that crack initiation was predominantly along the PE

ferrite boundary with pearlite (Figure 1); i.e. the higher the PE ferrite content, the lower the fatigue initiation life. Early crack growth involved ‘jumping’ between highly strained, PE ferrite zones, so as to accommodate the strain field. Detailed examinations, including nano-hardness tests within strain-hardened PE ferrite and pearlite, of sections from worn rail and test discs showed that there was strain partitioning between the PE ferrite and pearlite parts of the microstructure [1-3]. These observations have been used to refine the crack initiation and early growth modelling.

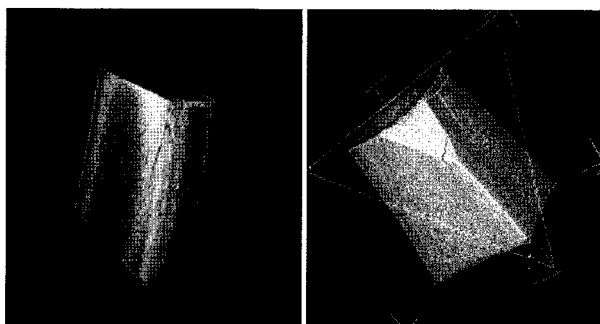


Fig. 2. X-ray Computed Micro-tomography Images of a Section Cut Around a Small RCF Crack in a Rail; Complete Section to Left and Section with Corner Slice Removed to Right

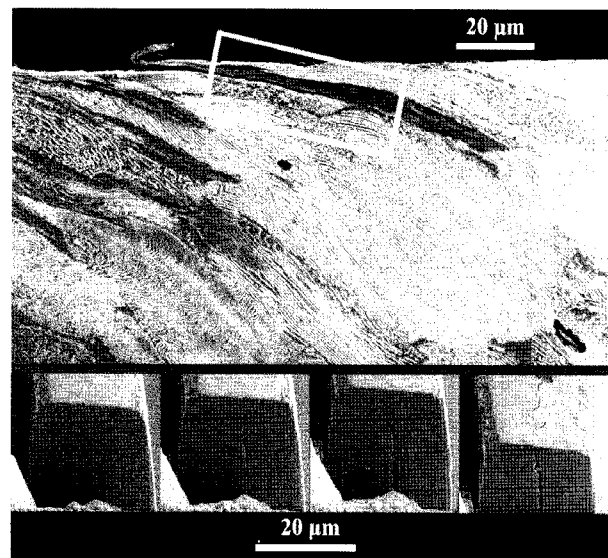


Fig. 3. FIB Examination of Crack Shapes Approaching the Tip of a Twin-disc Sample RCF Crack Shown in the 2-Dimensional Microsection (Top). The Rectangular Block Area (Outlined In The Top Image) was Extracted and Milled (from Right to Left) by FIB in One Hundred and Sixty, 0.25 μm Steps. The Bottom Images, Left to Right, at the 9.25, 12, 15 and 20 μm Stages Show the Crack Pattern Beneath the Crack shown on the (2D) Microsection, as the 2D Image Crack Tip is Approached

Some crack initiation was also observed on some highly strain-flattened ductile inclusions and at pearlite colony boundaries in near-fully pearlitic structures (i.e., minimal PE ferrite). Future work will involve looking at rail steels with minimal to zero PE ferrite.

The work described above led to consideration of crack initiation and growth in three dimensions (3D), as all microstructural observations so far had been two-dimensional (2D). For example, how is the 3D shape of the early initiating cracks determined, mainly by the strain field or by microstructural features such as PE ferrite boundaries. This has led to ongoing work examining 3D sections. Three methods have been used to date: (a) progressive grinding/polishing/micro-examination of selected cracks; (b) X-ray computed micro-tomography of a sample containing a small crack from a service rail and (c) focussed ion beam (FIB) examination of an area around a crack observed in 2D micro-sections. Methods 'b' and 'c' are far quicker than method 'a', but they do not reveal the microstructural detail (Figures 2 and 3).

These methods, together with standard metallurgical examination techniques, will facilitate further refinement of the modelling described below.

3. Ratcheting Model of Wear and Crack Initiation

The 'dynarat' computer simulation models plastic ratcheting of a ductile metal, leading eventually to wear and crack initiation. Plastic shear strain (γ) accumulates over thousands of load cycles, driven by the orthogonal shear stress (T_{zx} , see Figure 4). The deforming material is modelled as a mesh of elements (or 'bricks'), and each element can be assigned individual material properties, such

as initial hardness (proportional to the shear yield stress, k) and the critical plastic shear strain (γ_c) at which ductility is exhausted and 'failure' occurs. Strain hardening behaviour can be specified also. Material at the surface which fails can be removed as wear debris, and thus the wear rate over time (i.e., number of load cycles) can be predicted. Material which fails subsurface can be considered 'weak', unable to support tensile stresses and a potential site of crack initiation; the computer simulation can therefore estimate the number of load cycles until the initiation of a 'significant' crack. For example, the simulation might indicate for a specific load that cracks are likely to initiate to a depth of 0.5 mm after 25,000 cycles; separate crack propagation models could then predict further growth of such a crack. The ratcheting model theory is described in detail in Ref. [4].

Both 2D cases, such as twin-disc contact, and 3D cases, such as train wheel on rail, can be simulated. In 3D, a cross-section through the deforming material, parallel with the direction of motion, is simulated; however, the stresses acting on the elements are calculated by considering the contact in 3D. Since loading of rails is never known precisely, the model has been calibrated using twin-disc data from tests using British normal grade (Grade 220) rail steel and wheel steel disc samples, originally from Tyfour et al. [5] and more recently from Garnham et al. [2]. The latter collaboration also provided a large set of nano-hardness measurements of pearlite and PE ferrite which were used to develop microstructural models.

4. 3D Microstructural Modelling

In the ratcheting simulation, the material properties of each element can be selected to construct a representation

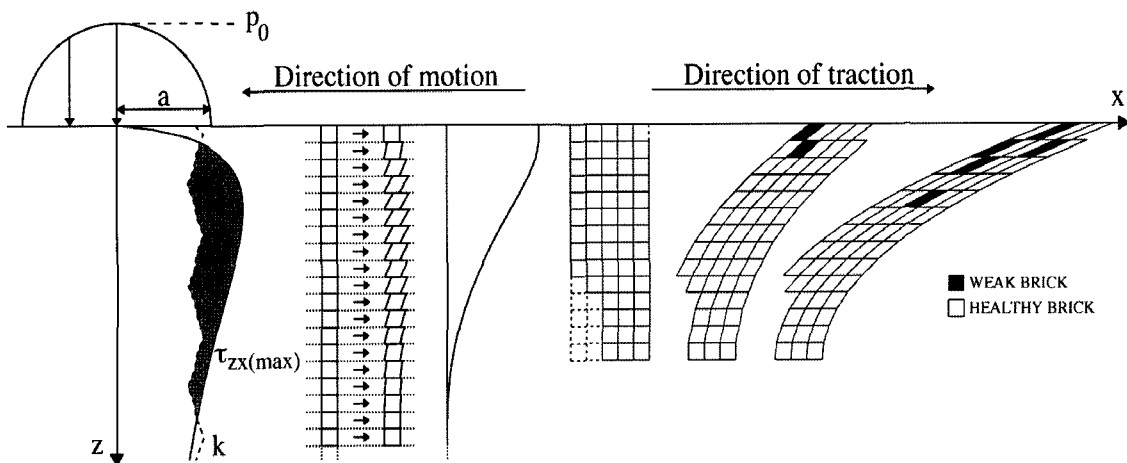


Fig. 4. Once the Rail Surface Shakes Down, Protective Residual Stresses form as a Result of Plastic Deformation. Subsequent Deformation is Driven by the Orthogonal Shear Stress, i.e., Plastic Deformation Occurs if the Maximum Value ($T_{zx(max)}$) Exceeds the Shear Yield Stress (k). This Deformation Builds Up over Thousands of Load Cycles until the Material's Ductility is Exhausted

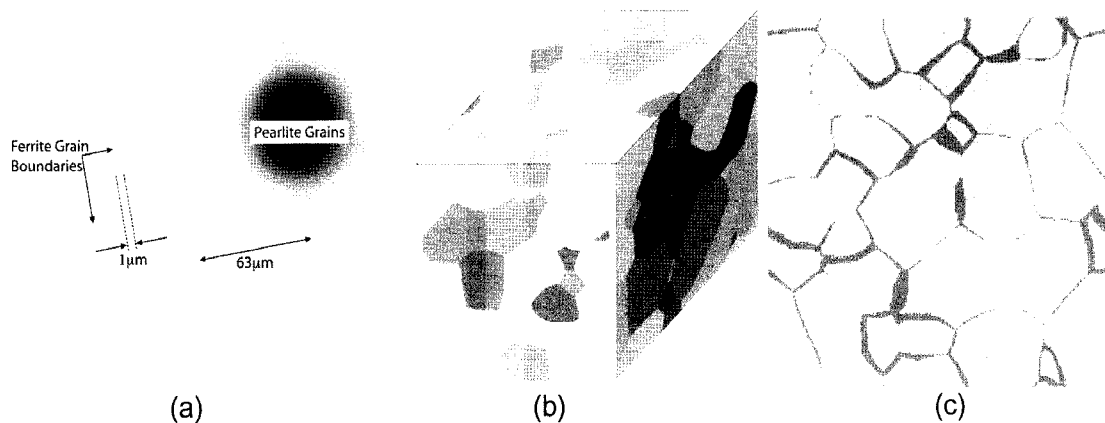


Fig. 5. (a) A Regular Hexagonal (2D) Microstructure which is Mathematically Simple and Easily Configurable. (b) A 3D Microstructure Generated by a Cellular Automaton; Different Colours Represent Different Orientations of Pearlite Colonies. (c) A More Realistic Microstructure Generated by Cross-section through the 3D Microstructure in (b); Light Grey Represents 'Pearlite' and Dark Grey Represents PE Ferrite at Prior-austenite Grain Boundaries

of rail steel microstructure. For example, elements can be assigned as 'pearlite' or PE ferrite according to a hexagonal pattern in which prior-austenite grain size, grain boundary width and grain orientation are configurable (see Figure 5(a)). This is a reasonable approximation of rail steel microstructure for the wear model and for indicating the probable depth of initiating cracks. However, to understand how cracks initiate and begin to grow in real steel microstructures, the regular and 2D nature of the hexagonal microstructure is not appropriate since barriers to crack growth are not represented.

Figure 5(b) shows a cube of microstructure which has been generated using a 3D cellular automaton (which uses random processes to 'grow' grains). The different colours represent different orientations of pearlite; different orientations will respond differently to shear stresses and deform in different ways. Given sufficient material data, this could be modelled by the ratcheting simulation. Generating the microstructure in this way, allows cross-sections to be taken through the cube, as shown in Figure 5(c), and this provides a much more representative microstructure than the regular hexagonal microstructure. (This is discussed further in Ref. [6].)

Another method for generating 3D microstructures is to use Voronoi polyhedra; this method is used by Nygård and Gudmundson [7], for example, and has the advantage that grains, etc., can be represented by their surfaces, making manipulation and graphical representation easier and reducing computation time. The surfaces are also the interfaces where crack initiation is likeliest to occur, so identification of potential crack paths through the microstructure (following plastic deformation as a result of ratcheting) is relatively easy and the probability of initiation of relatively long cracks can be assessed. This approach is cur-

rently in development.

Of course, representation of pearlitic rail steel as 'pearlite' grains with (prior-austenite) grain boundaries is overly simplistic. At the sub-grain level, standard pearlitic rail steel is a 3D composite of ferrite and cementite phases, plus non-metallic inclusions. Failure is dependent on how stress and strain are accommodated by these phases, inclusions and the bonds between them. This is being investigated using an elastic-plastic large strain deformation finite element study of the microstructure, which will provide property information at the micron level, with a detail impractical to measure experimentally.

5. Thermal Modelling

In the ratcheting model, the plastic shear strain of the material is driven by purely mechanical stress caused by normal and tangential loading, without thermoelastic effects. The effect on the mechanical stresses of partial slip, where the contact region is divided into 'stick' and 'slip' zones, can be simulated; for contacts which are fully slipping, the mechanical stresses are not affected by the slip speed, but thermal stress will develop because of frictional heating between the contact surfaces. Thermal stress in rolling/sliding contact between wheels and rails due to frictional heating can be the same order of magnitude as the mechanical stress [8-11], and the high temperature very close to the surface reduces the yield stress of the material in this region. The higher stress combined with the reduced yield stress is expected to cause early failure of the material, resulting in an increased wear rate and a greater propensity for crack initiation.

The elevated temperature, material softening and thermal stress, caused by frictional heating at the contact sur-

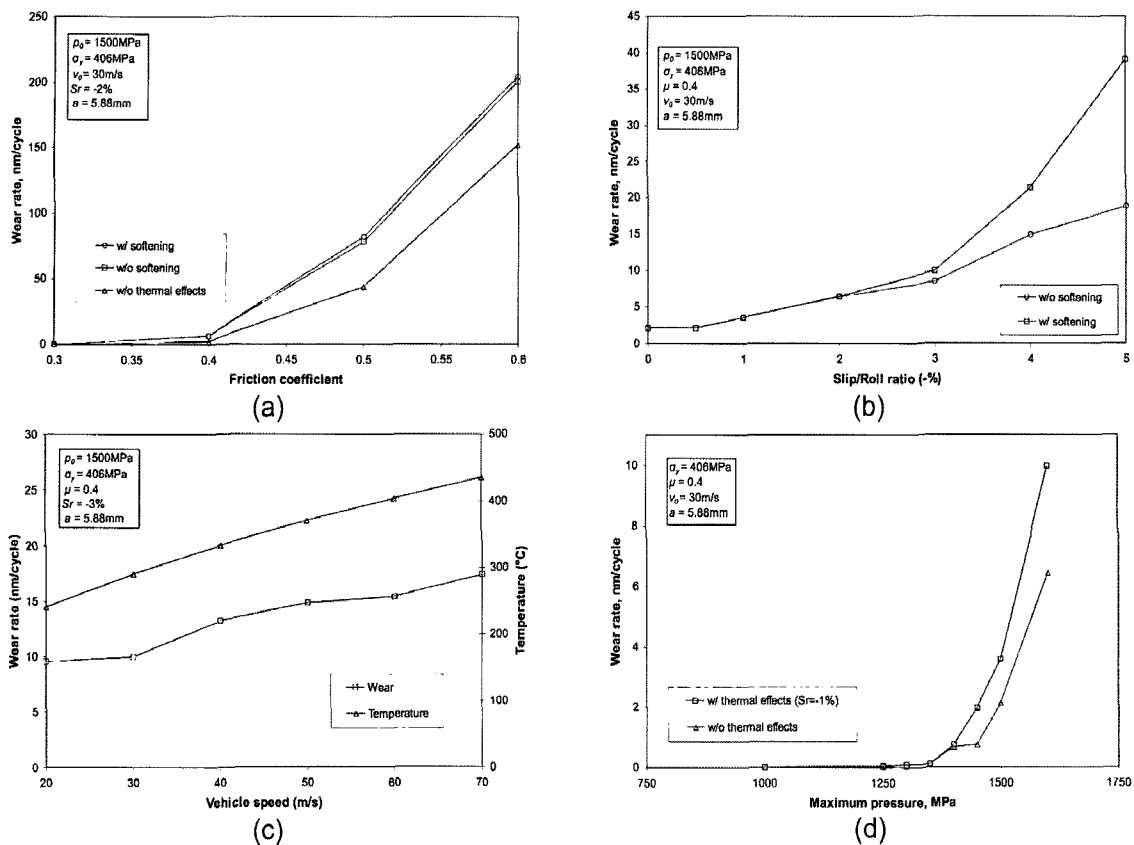


Fig. 6. Effect on Wear Rate of (a) Friction Coefficient, (b) Slip/roll Ratio, (c) Vehicle Speed, and (d) Peak Pressure. Results of Simulations Performed without Any Modelling of Thermal Effects ('w/o Thermal Effects') are Compared with Results of Simulations where Thermal Stresses are Considered with ('w/ Thermal Effects' or 'w/ Softening') and without Any Softening ('w/o Softening')

face, can be simulated using the 2D ratcheting model and the effects of operating conditions studied. Figure 6 shows the effect on the wear rate of varying friction coefficient, slip/roll ratio, vehicle speed, and peak pressure. Increasing the friction coefficient above 0.4, or increasing the peak contact pressure above about 1400 MPa, have the most marked impact on the wear rate, increasing it by orders of magnitude. Increasing the slip/roll ratio or the vehicle speed also increases the wear rate, although the latter result must be treated with some caution. Deters and Proksch [12] investigated the effect of rolling speed on wear rate and found that the volume of wear decreased with increasing rolling speed as a result of a slight decrease of the traction coefficient when the speeds of the roller increased.

6. Vehicle Sequences

The ultimate aim of the above simulation work is to be able to predict wear rates and time until fatigue crack initiation for a given rail steel, to provide guidelines for rail grinding in order to optimize rail life and safety. Once the

traffic for a particular location is known, multi-body simulation of train-track interaction (i.e., vehicle dynamics) can provide data on contact patch area (the contact patch between train wheel and rail is usually approximated as an ellipse) and contact stress, and this can be used as an input to the ratcheting simulation.

The two principal high speed trains operating on the East Coast Mainline (ECML) in the U.K. are the Intercity 125 (consisting of two Class 43 locomotives and about nine Mark 3 coaches) and the newer Intercity 225 (consisting of a Class 91 power car and trailer and nine Mark 4 coaches). During Rail Safety & Standards Board's Project T355, vehicle dynamics simulations were performed using VAMPIRE of these four vehicle types at two curves (at Harringay and Sandy) on the ECML, providing wheel-rail contact data for one wheel each on the high rail at three locations at these two sites (i.e., 4 vehicles \times 2 curves \times 3 locations = 24 contacts).

By grouping contacts for different vehicles it is possible to simulate the passage of trains, so that $2 \times 4 \times$ Class 43 + $9 \times 4 \times$ Mark 3 (a total of 44 wheel passes) represents an Intercity 125, and $2 \times 4 \times$ Class 91 + $9 \times 4 \times$ Mark 4 repre-

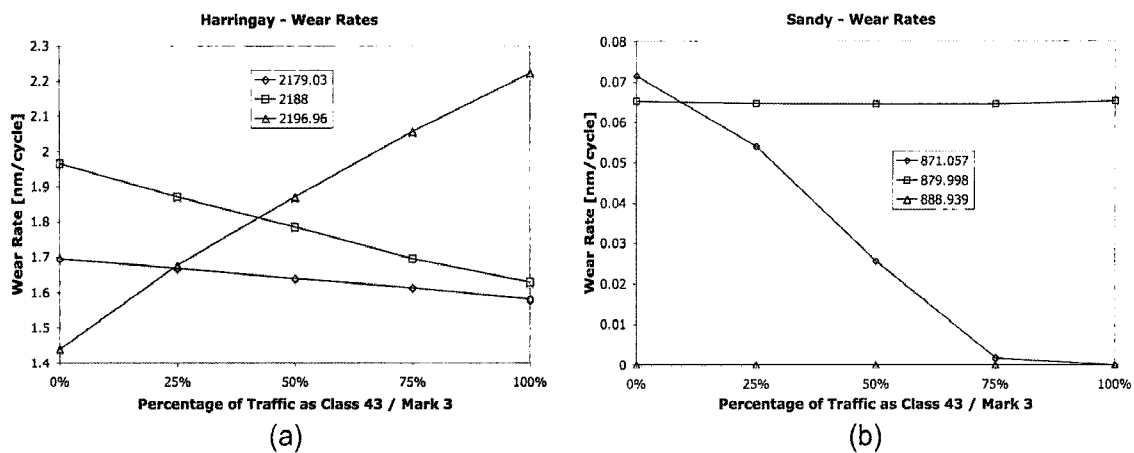


Fig. 7. Predicted wear Rates at (a) the Three Locations at Harringay, and (b) the Three Locations at Sandy. Only in One of the Six Cases does the Class 43/Mark 3 Combination (Intercity 125) Result in a Higher Wear Rate

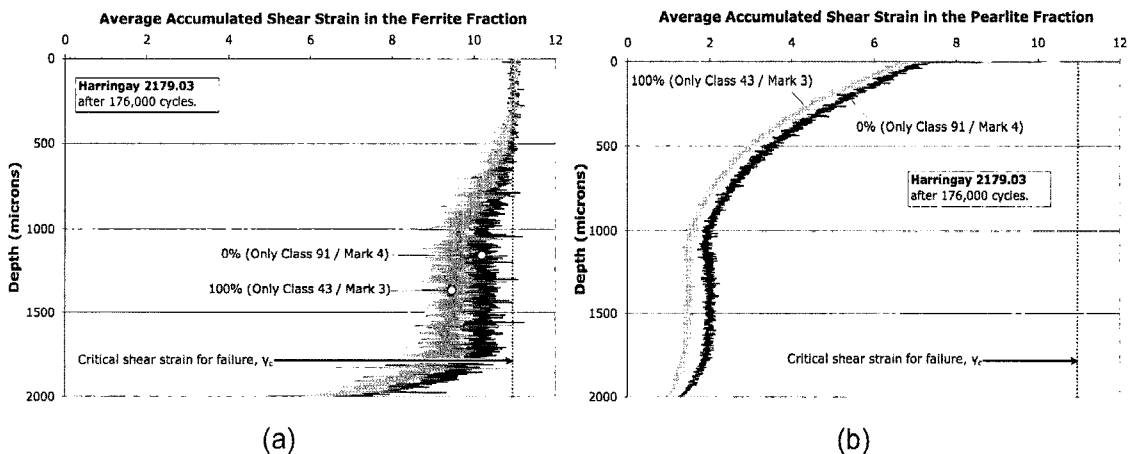


Fig. 8. From Simulations at One Location at Harringay: Accumulated Shear Strain with Depth, Averaged Across (a) the PE Ferrite, and (b) the Pearlite Elements Separately at Each Depth. When the Shear Strain Reaches the Critical Strain for Failure, Crack Initiation is This Region is Likely - Crack Initiation to a Depth of about 0.4 mm in the PE Ferrite is Likely at this Location

sents an Intercity 225. In this way it is also possible to model both trains and vary the proportion of each in the total traffic; variation of the predicted wear rates for different traffic mixtures is shown in Figure 7.

At each depth of the simulation, according to the microstructure model, a proportion of the elements have been given properties of ferrite, and the remainder have been given properties of pearlite. Figure 8 shows the accumulated shear strain, averaged at each depth separately over (a) the PE ferrite elements, and (b) the pearlite elements. Pearlite is harder than the PE ferrite and accumulates shear strain more slowly, so crack initiation is predicted sooner in the PE ferrite. For this location, the accumulated shear strain in the ferrite, down to about 0.4 mm depth, has reached the critical shear strain for failure, suggesting crack initiation to this depth is likely.

7. Conclusions

Prediction of rail life requires a multidisciplinary approach, and vehicle and track dynamics expertise is necessary just to provide the inputs, i.e., the wheel-rail contact data, to the modelling described in this paper. The ratcheting model can use this input data to predict wear and fatigue crack initiation for different vehicle mixtures at specific locations.

Central to rail life predictions is an understanding of how rail steel responds to forces - how it deforms plastically and how cracks initiate and grow. Metallurgical study of rail steel is producing high quality material data, and this is being incorporated into a new three-dimensional microstructure model which will allow study of short crack growth. Thermal effects are being incorporated into

the ratcheting model, which will lead to better predictions of the wear rate where there is a high degree of slip, such as at flange contacts.

Acknowledgements

The metallurgical investigation and microstructural modelling presented here are part of an ongoing collaborative development between the Universities of Birmingham and Newcastle as part of the EPSRC's Rail Research UK.

The wheel-rail contact data for Haringay and Sandy were provided to Newcastle University by Rail Safety and Standards Board during Project T355 "Management and Understanding of Rolling Contact Fatigue".

Corus Rail Technologies for supply and machining of materials, Carillion and Bombardier for materials, TWI for X-ray CIT support and the University of Loughborough for FIB test support.

Reference

1. H.C. Eden, J.E. Garnham, and C.L. Davis. "Influential microstructural changes on rolling contact fatigue crack initiation in pearlitic rail steels", *Materials Science and Technology*, Vol. 21, No. 6, pp. 623-629, (2007).
2. J.E. Garnham, F.J. Franklin, D.I. Fletcher, A. Kapoor, and C.L. Davis. "Predicting the life of steel rails", *Proc. IMechE, Part F: J. Rail and Rapid Transit (special issue)*, Vol. 221, No. 1 pp. 45-58, (2007).
3. J.E. Garnham and C.L. Davis. "The role of deformed microstructure on rolling contact fatigue initiation." *Proc. 7th Int. Conf. "Contact Mechanics and Wear of Rail/Wheel Systems," Brisbane, Australia, 24th-27th September, 2006*, pp. 399-409. [Accepted for publication in *Wear*, 2008.]
4. F.J. Franklin and A. Kapoor. "Modelling wear and crack initiation in rails", *Proc. IMechE, Part F: J. Rail and Rapid Transit (special issue)*, Vol. 221, No. 1 pp. 23-33, (2007).
5. W.R. Tyfour, J.H. Beynon, and A. Kapoor. "Deterioration of rolling contact fatigue life of pearlitic rail steel due to dry-wet rolling-sliding line contact", *Wear*, Vol. 197, pp. 255-265, (1996).
6. F.J. Franklin, J.E. Garnham, D.I. Fletcher, C.L. Davis, and A. Kapoor. "Modelling rail steel microstructure and its effect on wear and crack initiation", *Proc. 7th Int. Conf. "Contact Mechanics and Wear of Rail/Wheel Systems," Brisbane, Australia, 24th-27th September, 2006*, pp. 399-409. [Accepted for publication in *Wear*, 2008.]
7. M. Nygård and P. Gudmundson. "Three-dimensional periodic Voronoi grain models and micromechanical FE-simulations of a two-phase steel," *Computational Materials Science*, Vol. 24, pp. 513-519, (2002).
8. F.D. Fischer, E.A. Werner, and W.Y. Yan. "Thermal stresses for frictional contact in wheel-rail systems," *Wear*, Vol. 211, pp. 156-163, (1997).
9. A. Bohmer, M. Ertz, and K. Knothe. "Shakedown limit of rail surfaces including material hardening and thermal stresses," *Fatigue Fract. Eng. Mater. Struct.*, Vol. 26, pp. 985-998, (2003).
10. M. Ertz and K. Knothe. "Thermal stresses and shakedown in wheel/rail contact," *Archive of Applied Mechanics*, Vol. 72, pp. 715-729, (2003).
11. T. Goshima and L.M. Keer. "Stress intensity factors of a surface crack in semi-infinite body due to rolling-sliding contact and frictional heating," *Trans. Jpn. Soc. Mech. Eng.*, Vol. 56, No. 532, pp. 2567-2572, (1990).
12. L. Deters, M. Proksch. "Friction and wear testing of rail and wheel material," *Wear*, Vol. 258, pp. 981-991, (2005).